Thermal Behavior of Fluorinated Aromatic Polyethers and Poly(ether ketone)s

A. A. Goodwin,*,† F. W. Mercer,‡ and M. T. McKenzie‡

Department of Materials Engineering, Monash University, Clayton, Victoria 3168, Australia, Raychem Corporation, Research and Development, Menlo Park, California 94025

Received May 8, 1996; Revised Manuscript Received December 9, 1996[⊗]

ABSTRACT: Eight amorphous polyethers and poly(ether ketones) were synthesized and characterized by gel permeation chromatography, thermogravimetric analysis, differential scanning calorimetry, and dynamic mechanical thermal analysis. Polymers containing bulky, cyclic 2,2′-biphenyl side groups were found to have the highest glass transition temperatures, were more thermally stable and exhibited the highest intramolecular barriers to rotation. Incorporation of perfluorophenylene groups resulted in internal plasticisation and a relative lowering of T_g. The steepness of cooperativity plots determined from Williams−Landel−Ferry shift factors correlated with the rigid nature of the polymer chains, but not with the broadness of the relaxation (characterized by the Kohlrausch−Williams−Watts stretch exponent β) as predicted by the coupling model. A β-process observed in the polymers containing cyclic biphenyl side groups was similar in appearance to a typical "structural" relaxation. The position, intensity, and breadth of the γ-process was sensitive to chemical structure and absorbed moisture.

Introduction

Linear aromatic polymers have long been known for their usefulness in meeting the high-performance requirements for structural resins, polymer films, and coating materials needed by the aerospace and electronics industry. Aromatic polyimides[1,2] and poly(ether ketone)s[3−6] are the polymers of choice for these applications because of their unique combination of chemical, physical, and mechanical properties. In addition, because of the flexible ether and ketone groups present in the polymer backbone, poly(aryl ether ketone)s are generally more easily processed than polyimides.

Considerable attention has also been devoted to the preparation of fluorine-containing polymers because of their unique properties and high-temperature performance. Among the high-performance fluorinated polymers being studied for use in aerospace and electronic applications are the fluorinated aromatic polyethers prepared containing hexafluoroisopropylidene (HFIP) units.[7] Polymers containing HFIP units have been studied for applications as films, as coatings for optical and microelectronics devices, as gas separation membranes, and as matrix resins in fibre reinforced composites. Frequently the incorporation of HFIP units into the polymer backbone leads to polymers with increased solubility, flame resistance, thermal stability, and glass transition temperature, while also leading to decreased color, crystallinity, dielectric constant, and moisture absorption.

Recently we reported on the synthesis and characterization of novel fluorinated poly(aryl ether)s containing perfluorophenylene moieties.[8] These fluorinated polyethers were prepared by reaction of decafluorobiphenyl with bisphenols. These polymers exhibit low dielectric constants, low moisture absorption, and excellent thermal and mechanical properties. Tough, transparent films of the polymers were prepared by solution casting or compression molding. The fluorinated poly(aryl ether)s containing perfluorophenylene moieties are good candidates for use as coatings in microelectronics applications.[9]

Thermal and relaxation studies of high-performance thermoplastics have mainly focused on amorphous and semicrystalline poly(ether ether ketone) (PEEK) which has a glass transition temperature of 143 °C and a melting point temperature around 340 °C. It is commonly studied for its structure/property relations since wide variations in morphology can be achieved by controlling the thermal history.[10] Dynamic mechanical studies of amorphous PEEK reveal an α-relaxation associated with the glass transition and a bimodal sub-T_g β-relaxation, at around −100 °C, which is associated with local chain motions.[11] A γ-transition has also been detected at −150 °C.[12] In crystalline samples, the α-relaxation is raised in temperature and significantly broadened, compared with that of the amorphous polymer. This is attributed to constraints imposed by the crystallites on the segmental mobility of the amorphous regions.[13] The bimodal nature of the β-relaxation has been attributed to cooperative, as well as noncooperative, motions and is sensitive to water content, morphology, and aging history.[14]

In this paper we report on the thermal behavior of a series of aromatic polyethers and poly(ether ketone)s into which cyclic 2,2′-biphenyl side groups, HFIP, perfluorophenylene, and oxadiazole groups have been incorporated.

Experimental Section

Materials. Illustrative synthetic procedures used in this study are described below. Details of the synthetic methods used to prepare the remaining polymers can be found elsewhere.[15,16]

Polymer **3a** was prepared from decafluorobenzophenone and 9,9-bis(4-hydroxyphenyl)fluorene using the following general procedure. A typical synthesis of the fluorinated polyether-ketone was conducted in a 100 mL round bottom flask equipped with a condenser, magnetic stirrer, and nitrogen inlet. To a 100 mL round bottom flask was added 6.19 g (0.017 mol) of decafluorobenzophenone, 5.77 g (0.017 mol) of 9,9-bis-(4-hydroxyphenyl)fluorene, and 45 g of DMAc. The mixture was stirred until all the solids dissolved, then 6.2 g (0.045 mol)

* Author to whom correspondence should be addressed: e-mail, goodwin@eng.monash.edu.au.
† Department of Materials Engineering.
‡ Research and Development.
⊗ Abstract published in *Advance ACS Abstracts,* April 1, 1997.

S0024-9297(96)00676-6 CCC: $14.00

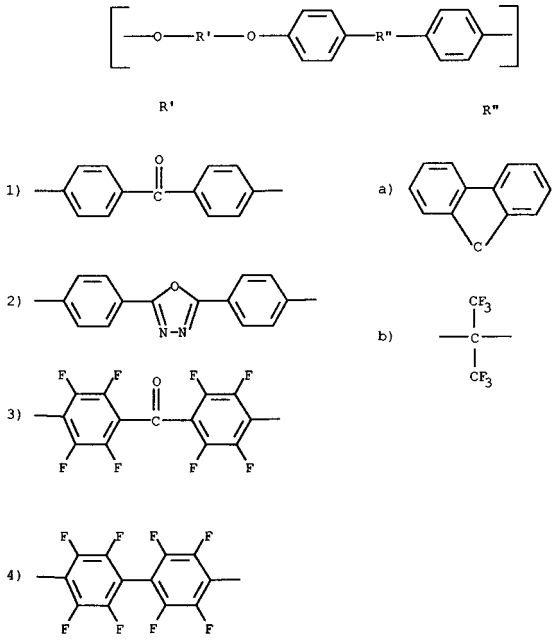

Figure 1. Chemical structures of aromatic polyethers and poly(ether ketone)s.

of potassium carbonate was added. The mixture was then heated to 160 °C and stirred under nitrogen for 3 h. The mixture was allowed to cool to room temperature and poured into rapidly stirring (in a blender) deionized water containing 1 wt % acetic acid to precipitate the polymer. The polymer was isolated by filtration, washed twice with deionized water, and dried to yield the fluorinated polymer as a white powder.

A general synthetic method designed to prepare **1a** and **1b** from difluorobenzophenone and diphenols was carried out using the following procedure. The synthesis of the polyetherketones **1a** and **1b** was conducted in a 50 mL round bottom flask equipped with a condenser, magnetic stirrer, and nitrogen inlet. Polymer **1b** was prepared from 4,4′-difluorobenzophenone and 4,4-(hexafluoroisopropylidiene)diphenol using the following procedure. To a 50 mL round bottom flask was added 1.5 g (0.0069 mol) of 4,4′-difluorobenzophenone, 2.31 g (0.0069 mol) of 4,4-(hexafluoroisopropylidiene)diphenol, and 25 g of dry *N*,*N*-dimethylacetamide (DMAc). The mixture was stirred until all the solids dissolved, then 2.2 g (0.016 mol) of potassium carbonate was added. The mixture was then heated to 160 °C and stirred under nitrogen for 32 h. The mixture was allowed to cool to room temperature, and it was then poured into rapidly stirring (in a blender) deionized water containing 1 wt % acetic acid to precipitate the polymer. The polymer was isolated by filtration, washed twice with deionized water, and dried to yield the polymer as a white powder.

The structures of the polymers investigated here are shown in Figure 1.

Gel Permeation Chromatography. The molecular weight results were generated using a Waters 150C gel permeation chromatography (GPC) instrument operated at 60 °C. Solutions of the polymers were prepared in a nuclear microprobe (NMP) containing 0.05M LiBr. Solution concentrations were 10 mg/10 mL in a NMP. Separation was accomplished using 3×10 μm mixed-B columns from Polymer Labs. The results are the average of two injections of each solution. Calibration was performed using narrow polydispersity polystyrene standards.

Thermogravimetric Analysis. Thermogravimetric analysis (TGA) of each of the polymers was performed on a Seiko SSC 5200 System DSC 220C TGA/DTA 320. Analysis was carried out in air at a heating rate of 20 °C/min. TGA decomposition temperatures in air were characterized as being the temperature where a 5 wt % loss was observed. For isothermal heat aging, samples were heated to the desired temperature at a rate of 20 °C/min and held at either 400 or 450 °C for 3 h in air.

Differential Scanning Calorimetry. Prior to analysis the polymers were compression molded into thin sheets at temperatures above their respective glass transitions. Samples weighing approximately 10 mg were cut from the sheets and scanned in a Perkin-Elmer differential scanning calorimeter, Model DSC7. All samples were first held at 300 °C for several minutes to erase any previous thermal history before rapidly cooling to 100 °C. The T_g was then determined by scanning to 300 °C at 10 °C/min, with the T_g taken as the midpoint of the change in slope of the heat flow/temperature plot. The temperature and power response of the calorimeter were calibrated using high-purity indium and zinc. No transitions due to crystallization or melting were detected in any of the samples.

Dynamic Mechanical Thermal Analysis. The dynamic mechanical response of the samples was monitored using a Rheometric Scientific DMTA MKII in the bending mode, with dual cantilever geometry. Rectangular samples, measuring 30 mm × 10 mm × 0.2 mm, were scanned isochronally at 2 °C/min between −120 and 300 °C and isothermally around the glass transition. Loss modulus (E''), storage modulus (E') and tan δ were recorded over the frequency range 0.03−200 Hz. All experiments were carried out in an inert atmosphere on the samples cut from compression molded sheets.

Curve Fitting. Nonlinear least-squares-curve-fitting of the dynamic mechanical loss curves was accomplished by the use of the commercial PeakFit software (Jandel Scientific) which uses the iterative Marquardt−Levenberg fitting algorithm. This involves estimating values for the adjustable parameters such that the function

$$\chi^2 = \sum_{i=0}^{n}\left[\frac{\mathrm{f}(x_i - y_i)}{\sigma_i}\right]^2 \qquad (1)$$

is minimized, where $y = f(x)$, with f representing a model fitting function, and σ is standard deviation. This procedure provides values for the adjustable parameters such that the fitting function is optimum in a least-squares sense. A fit is converged when χ^2 is unchanged within the eighth significant figure for five full iterations. The confidence intervals for the model parameters are determined at the 95% limit using a method outlined by Draper and Smith.[17] A graphical prefitting method was used to manipulate the fitting function on the screen to match the experimental data as closely as possible prior to fitting.

All other fitting procedures were achieved using Sigma Plot (Jandel Scientific).

Results and Discussion

Polymer Synthesis. All the polymers described in this paper were prepared by the nucleophilic aromatic substitution of an aryl halide with a phenoxide. Aryl halides, when activated by an electron-withdrawing substituent (such as ketone, oxadiazole, perfluoroaryl, etc.) which can accept a negative charge, are susceptible toward nucleophilic aromatic substitution polymerizations. Polycondensation reactions of the aryl halides with diphenols were carried out in DMAc at 160 °C using an excess of potassium carbonate as base. Aqueous workup of the reaction mixtures yielded the polymers as white powders. The isolated polymers were thoroughly washed with water to remove the residual DMAc and potassium salts. Size exclusion chromatography was used to determine the molecular weight of each polymer and the results are listed in Table 1. The molecular weight distributions were essentially unimodal with no evidence of oligomeric or unreacted species. The reported values are polystyrene equivalent weights. The actual molecular weights of these materials may be greater. Regardless, the molecular weights are consistent with the ability to form tough, flexible films.

Table 1. of Aromatic Polyethers and Poly(ether ketone)s of Aromatic Polyethers and Poly(ether ketone)s

sample	M_w (g/mol)	M_n (g/mol)	M_z (g/mol)	M_w/M_n	TGA onset[a] (°C)	DSC T_g (°C)	DMTA T_g (°C)
1a	78 000	26 000	197 000	3.0	516	234	249
1b	102 000	39 000	229 000	2.6	472	159	173
2a	60 000	26 000	101 000	2.3	475	267	282
2b	44 000	20 000	72 000	2.2	465	192	206
3a	39 000	14 000	81 000	2.8	436	216	236
3b	38 000	14 000	84 000	2.7	425	149	160
4a	71 000	30 000	128 000	2.4	500	248	262
4b	39 000	19 000	63 000	2.1	500	167	182

[a] Onset of decomposition in air.

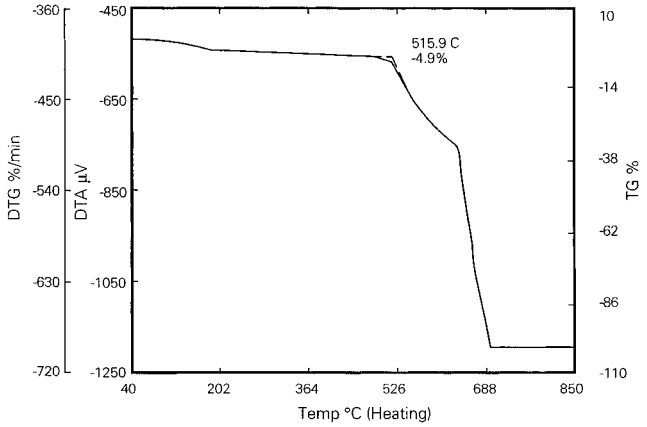

Figure 2. TGA heating scan of **1a**.

Thermogravimetric Analysis. A typical thermogravimetric analysis (TGA) trace is shown in Figure 2. TGA results are presented in Table 1. In isothermal aging experiments, **4a** experienced a weight loss of 2.7% and 3.6% when held for 3 h in air at 400 and 450 °C, respectively, while **4b** experienced a weight loss of 2.5% and 19.8% under the same conditions. Generally, the polymers containing the cyclic biphenyl side groups prepared using 9,9-bis(4-hydroxyphenyl)fluorene are more stable than those containing the HFIP groups prepared with 4,4′-(hexafluoroisopropylidiene)diphenol.

Glass Transition Temperatures. There are some interesting trends in the T_g's of these materials which can be related to polymer structure. For example, a comparison of the DSC results in Table 1 for **1b** and **3b** shows that incorporation of perfluorophenylene groups results in a relative lowering of T_g by 10 °C. This probably occurs as a result of internal plasticization and disruption in chain packing due to the bulky aromatic fluorine atoms, as well as a reduction in the chain polarity of **3b**, compared with **1b**. This arises from the electronegative character of fluorine acting to lower the polarizability of neighboring aromatic ketone groups. This idea is supported by earlier studies which have shown that incorporation of fluorine into a polyimide backbone reduces the dielectric constant, which is a function of chain polarity.[18,19] Incorporation of hexafluoroisopropylidene linkages in the poly(ether ketone) chain (sample **1b**) does produce a positive offset in T_g compared with PEEK. Polyether **4b** differs from sample **1b** insofar as it does not possess a ketone connecting group. The effect of this is to increase the chain stiffness and increase the differential scanning calorimetry (DSC) T_g from 159 °C to 167 °C. Polymer **2b** has an oxidiazole connecting group which has a greater positive effect on chain polarity than a ketone connecting group and the DSC T_g of this polymer is increased to 192 °C, compared with 159 °C for **1b**.

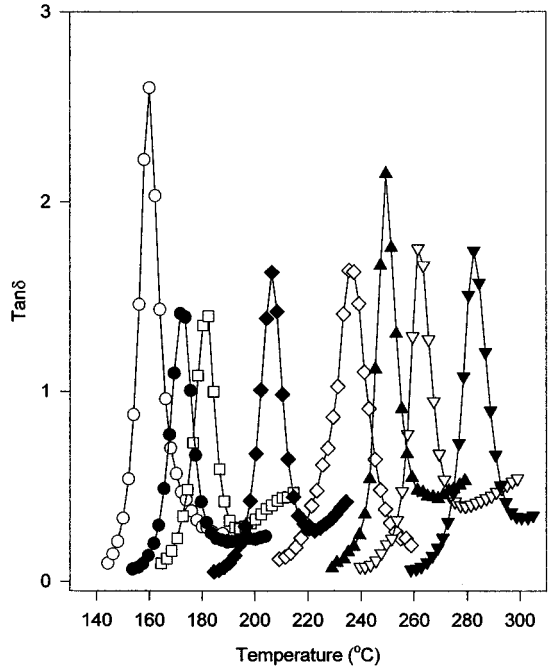

Figure 3. Temperature dependence of DMTA tan δ in α-relaxation region. Data are taken from isothermal experiments. **1a** (▲), **1b** (●), **2a** (▼), **2b** (◆), **3a** (◇), **3b** (○), **4a** (▽), **4b** (□).

The remaining polymers possess T_g's in excess of 200 °C which results from the steric hindrance caused by the cyclic biphenyl side groups. The polymer with the highest T_g (**2a**) is a polyether and contains a polar oxidiazole group. There is a relative lowering of T_g in sample **3a**, compared with the lowering of T_g's of samples **1a** and **4a**, since **3a** contains both perfluorophenylene and ketone groups.

Calculations have predicted that poly(aryl ether)s have quite flexible backbones and, as such, have values of entanglement molecular weight that are below 10 000 g/mol[42] while GPC and DSC studies on phosphorus containing aromatic polyethers[43] have shown the critical value to be around 15 000 g/mol. These values are below the molecular weights of the polymers we have studied and therefore we can expect that the glass transition temperatures are insensitive to changes in molecular weight within this range.

α-Relaxation. The dynamic mechanical thermal analysis (DMTA) responses of each polymer, around the glass transition at 1 Hz, are shown in Figure 3. All samples exhibit a relatively narrow, α-relaxation peak which corresponds to the glass transition and reflects the onset of large scale chain motions. The maximum in tan δ values range from 1.3 to 2.5, with the temperature corresponding to the maximum in tan δ being defined as the glass transition temperature.

The dynamic mechanical and DSC T_g's are listed in Table 1. The dynamic mechanical T_g's are between 11 and 20 °C above those measured by DSC which is a consequence of the higher effective measuring frequency of DMTA. The logarithmic frequency dependence of the dynamic mechanical glass transition temperatures are plotted in Figure 4. Such plots are commonly fitted to the empirical Volger−Fulcher equation, which describes the temperature dependence of relaxation times obtained from mechanical, dielectric, and other techniques for probing molecular motions at the glass transition.[20]

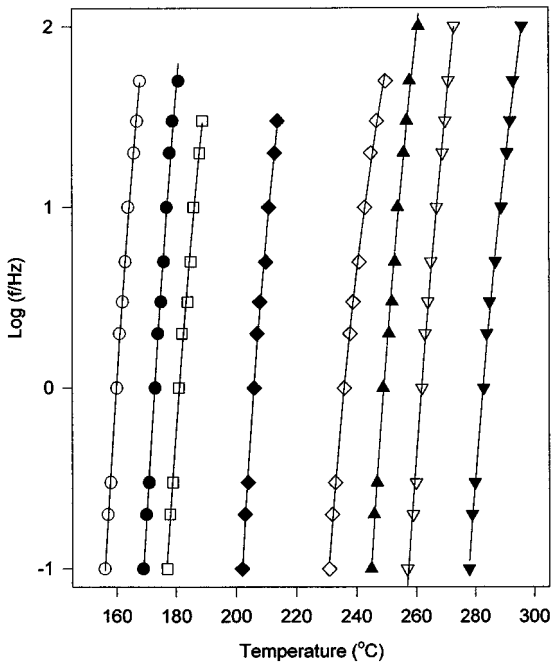

Figure 4. Temperature dependence of relaxation behavior in α-relaxation region. Solid lines are fits to Vogel−Fulcher equation, **1a** (▲), **1b** (●), **2a** (▼), **2b** (◆), **3a** (◇), **3b** (○), **4a** (▽), **4b** (□).

Table 2. Vogel−Fulcher and Arrhenius Parameters for Aromatic Polyethers and Poly(ether ketone)s

sample	log (f_o/s)[a]	E_{vf} (kJ/mol)[a]	T_o (°C)[a]	E_{Arr} (kJ/mol)[b]
1a	11.6 ± 2.7	11.9 ± 5.7	195 ± 14	1019 ± 29
1b	14.9 ± 6.4	17.0 ± 14.9	113 ± 27	905 ± 26
2a	10.5 ± 2.1	11.4 ± 4.9	226 ± 13	993 ± 28
2b	7.6 ± 1.8	4.9 ± 2.9	172 ± 9	901 ± 34
3a	6.6 ± 0.7	4.9 ± 1.2	197 ± 5	723 ± 30
3b	12.2 ± 2.8	11.8 ± 5.3	109 ± 12	813 ± 19
4a	13.9 ± 4.4	17.6 ± 11.4	196 ± 23	1063 ± 29
4b	10.9 ± 5.0	10.6 ± 4.2	131 ± 24	807 ± 27

[a] Fits to eq 2. [b] Calculated using Arrhenius equation.

The Vogel−Fulcher equation is given by

$$\log f^* = \log f_o - \frac{E_f}{2.303R(T - T_o)} \qquad (2)$$

where f^* is the frequency corresponding to temperature T from the mechanical loss peak, f_o is the primitive frequency at the Vogel temperature, T_o (the relaxation time τ is defined as $1/2\pi f$) where the entropy of the system approaches zero and E_{vf} is an energy term related to bond rotational barriers. The Vogel−Fulcher parameters are listed in Table 2. The energy term E, which is of the order of bond rotational barriers, is identical, within experimental error, for all polymers. Previous studies on flexible polymers,[21] for example, poly(methyl methacrylate) and poly(ethylene oxide), found E to be of the order of 3 kJ/mol. The higher values found in this study result from the rigid aromatic nature of these polymers. Similarly, it is not possible to discriminate between values of the primitive frequency log f^* as a result of the experimental error of the curve fits. The trend in the Vogel temperature T_0 is consistent with the trend in glass transition temperature of each polymer and is generally around 50 °C below the DSC T_g.

To compare with alternative functions, the plots in Figure 4 were also fitted to the Arrhenius equation to determine an apparent activation energy, E_{Arr}, the values of which are also listed in Table 2. The trend in activation energy here is such that three of the four polymers containing cyclic biphenyl side groups (**1a**, **2a**, and **4a**) have significantly larger values of E_{Arr}, compared with those of the remaining polymers. From a consideration of the size of the cyclic biphenyl side groups, it would be expected that the barriers to rotation around the main chain would be high in such polymers. The exception is **3a** which also contains perfluorophenylene groups and a ketone connecting group. This polymer has the lowest Arrhenius activation energy of the polymers studied here. It should be noted that since the plots in Figure 4 show slight curvature the values of E_{Arr} determined using the Arrhenius equation are linear approximations.

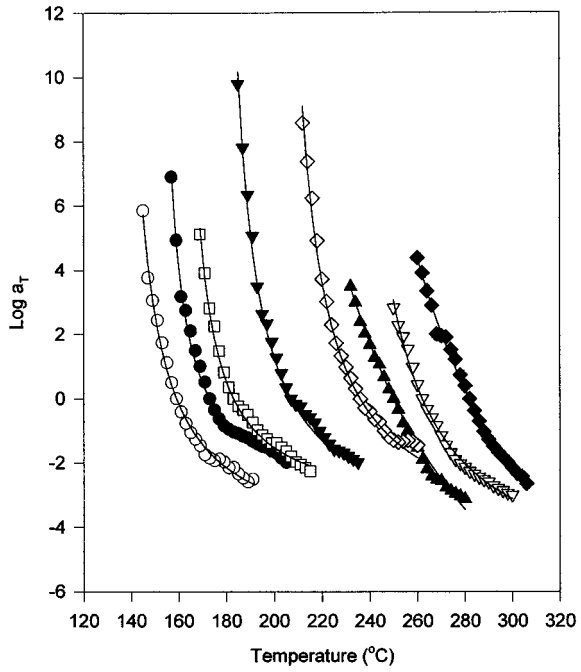

Figure 5. Temperature dependence of WLF shift factor, a_T. Solid lines are fits to WLF equation, **1a** (▲), **1b** (●), **2a** (▼), **2b** (◆), **3a** (◇), **3b** (○), **4a** (▽), **4b** (□).

The temperature dependence of viscoelastic relaxation times can also be described by the Williams−Landel−Ferry (WLF) equation[23] given by

$$\log a_T = \log\left(\frac{\tau^*}{\tau_R^*}\right) = \frac{-C_1(T - T_R)}{C_2 + T - T_R} \qquad (3)$$

where a_T is a shift factor, τ^* and τ_R^* are the relaxation times at temperatures T and T_R, respectively, and C_1 and C_2 are constants. The shift factors a_T, for all of the polymers in this study, were determined from isothermal plots of the dynamic mechanical log E' against temperature. This is a useful method for obtaining time−temperature superposition data over a wide temperature range. The temperature dependence of log a_T is shown in Figure 5 for each of the polymers with the corresponding WLF fits listed in Table 3. The WLF constants can be recalculated for the calorimetric T_g using[24]

$$C_1 = \frac{C_{1g}C_{2g}}{C_{2g} + T_R - T_g} \qquad (4)$$

$$C_2 = C_{2g} + T_R - T_g \qquad (5)$$

where C_{1g} and C_{2g} are the WLF constants at T_g.

Table 3. WLF Parameters for Aromatic Polyethers and Poly(ether ketone)s (from Fits to Eq 3)

sample	C_1	C_2 (K)	T_R (°C)
1a	13.5 ± 1.1	88.0 ± 7.3	250
1b	3.3 ± 0.1	23.6 ± 0.4	173
2a	12.3 ± 1.0	83.9 ± 6.0	282
2b	4.5 ± 0.2	31.7 ± 0.5	207
3a	4.6 ± 0.3	36.1 ± 0.8	236
3b	4.8 ± 0.2	25.7 ± 5.4	159
4a	6.0 ± 0.2	35.6 ± 1.3	262
4b	3.6 ± 0.1	23.6 ± 0.5	183

Table 4. WLF Parameters at T_g and Relaxation Strength for Aromatic Polyethers and Poly(ether ketone)s

sample	C_{1g}[a]	C_{2g} (K)[a]	T_o (°C)[b]	$E_a(T_g)$[c] (kJ/mol)	E[d] (kJ/mol)	S[e]
1a	16.5	72	162	240	22.8	9.1
1b	8.1	9.6	149	408	1.5	7.4
2a	15	68.9	198	297	19.8	6.7
2b	8.5	16.7	175	359	2.7	7.4
3a	10.3	16.1	200	572	3.2	6.7
3b	7.9	15.7	133	214	2.4	10.7
4a	9.9	21.6	226	540	4.1	7.6
4b	11.2	7.6	159	787	1.6	5.7

[a] Fits to eqs 4 and 5. [b] $T_o = T_g - C_{2g}$. [c] Calculated using eq 6. [d] Calculated using eq 7. [e] Calculated using eq 9.

The apparent activation energy at T_g, $E_a(T_g)$, follows a temperature dependence such that[24]

$$E_a(T_g) = \frac{2.303RC_{1g}(T_g)^2}{C_{2g}} \quad (6)$$

At high temperatures the intramolecular, or primitive, activation energy, which is associated with local barriers opposing rotation, is calculated from[24]

$$E = 2.303RC_{1g}C_{2g} \quad (7)$$

The parameters C_{1g}, C_{2g}, $E_a(T_g)$, and E calculated using the above relations are presented in Table 4 along with the Vogel temperature T_0 which is given by $T_0 = T_g - C_{2g}$. Although there appears to be no identifiable trend within the values of $E_a(T_g)$, there is a clear trend in the values of the primitive activation energies. **1a** and **2a** possess significantly higher values of E, compared with those of the other samples, while **4a** and **3a** display values much lower than those of **1a** and **2a**, but greater than those of the other samples. These findings are consistent with those from the Arrhenius analysis and confirm that the cyclic biphenyl side groups have a significant effect on mechanical relaxation in these materials by increasing intramolecular rotational barriers, while the incorporation of perfluorophenylene groups in **4a** and **3a** produces a relative lowering of intramolecular barriers. This is perhaps associated with the internal plasticising effects of perfluorophenylene groups which also confers a relative lowering of T_g.

The relative temperature dependence of the shift factors for these systems is not easily observed from Figure 5 since the glass transition shifts with molecular structure and molecular mobility scales with the distance of the experimental temperature from the DSC T_g. Therefore, it is more revealing to normalize the data using an arbitrary temperature, $T\alpha$, which is taken from outside the measuring range—often the DSC T_g or the temperature at which the relaxation time is equal to a particular value is used. For low molecular weight glasses, plots of relaxation time (or the equivalent frequency) against $T\alpha/T$ are referred to as fragility plots, whereas for polymers they are more commonly known as cooperativity plots.[22] Figure 6 shows the WLF shift factors replotted as a cooperativity plot for **1b** and **4a**, using the calorimetric T_g as a normalizing factor. This enables relative changes in the temperature dependence of the shift factors to be more easily observed. The coupling model of Ngai and co-workers[25] relates the temperature dependence of relaxation times to the extent of intermolecular cooperativity, which in turn correlates with chemical structure. Specifically, the more rigid and inflexible a polymer backbone is, the more coupled it is to the motions of its near neighbors, and the steeper its time and temperature dependence will be. Figure 6 shows that both polymers exhibit non-Arrhenius behavior which is indicative of strong coupling and that **4a**, which contains a cyclic biphenyl side group, has the greater degree of intermolecular coupling. In general, the polymers containing this rigid side group had steeper cooperativity plots. The coupling model also relates relaxation broadness to intermolecular coupling through the coupling parameter n, which is related to the Kohlrausch–Williams–Watts (KWW) broadness parameter β_{kww} by $\beta_{kww} = 1 - n$. As n increases, β_{kww} decreases and the relaxation spectrum broadens. In terms of the coupling model the strength of intermolecular coupling is proportional to n.[22]

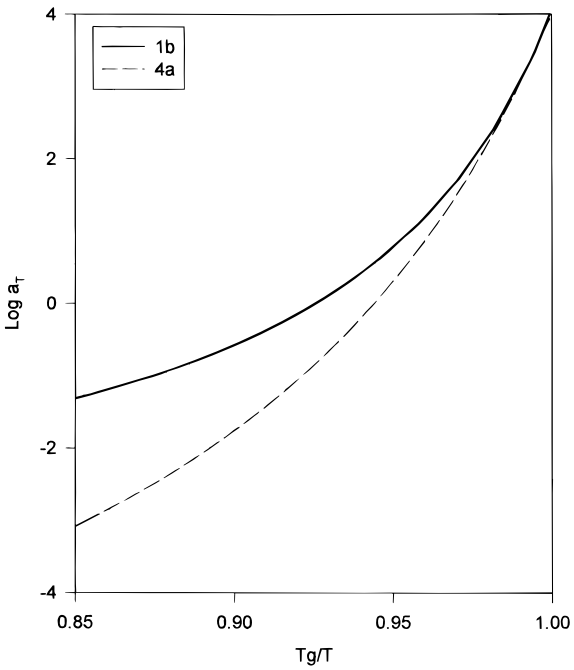

Figure 6. Cooperativity plot of WLF shift factors normalized by T_g at which log $a_T = 4$: **1b** (—), **4a** (– –).

The normalized plots of mechanical loss E'' for **1b** and **4a**, which are shown in Figure 7, were constructed using the WLF shift factors presented in Figure 5. This procedure resulted in satisfactory time/temperature superposition of loss curves. The solid lines are curve fits to the well-known Havriliak–Negami function.[26] The shifted curves were also fitted to the KWW function[27] (given below):

$$\phi(t) = \exp(-t/\tau^*)^{\beta} \quad (8)$$

using the Fourier transform method developed by Moynihan et al.[28] In eq 8, τ is a characteristic relaxation time and β_{kww} is related to the broadness of the relaxation. The values of β_{kww}, calculated for each

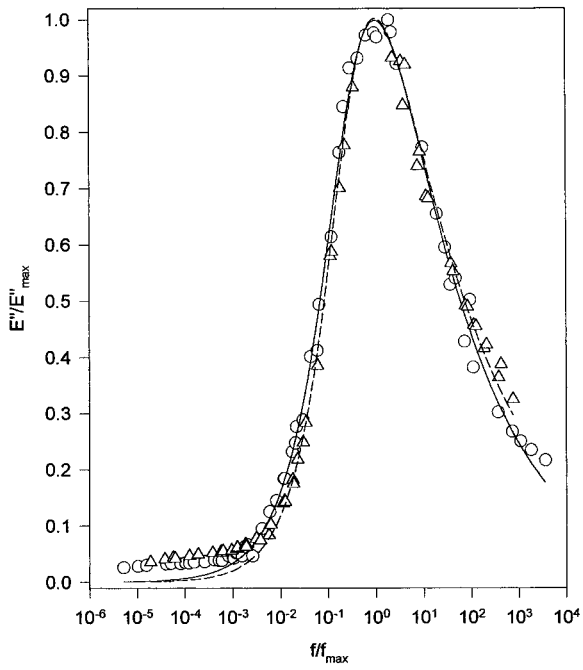

Figure 7. Normalized isothermal mechanical loss E'' plots constructed using WLF shift factors. Solid lines are fits to Havriliak−Negami equation: **1b** (○), **4a** (△).

polymer, varied between 0.32 and 0.36 (±0.3) for **1b**, **2b**, **3a**, and **4a** and between 0.42 and 0.48 (±0.3) for **1a**, **2a**, **3b**, and **4b**. These findings suggest that there is no simple correlation between molecular structure and relaxation broadness. Similarly, there is no correlation between the steepness of the cooperativity plots and spectral broadness, as anticipated by the coupling model. This indicates that an alternative explanation is required to describe the temperature dependence of relaxation times in these polymers. A recent study of substituted rigid polyphenylenes by Connolly et al.[29] also found a lack of correlation between coupling and time/temperature dependence. In this case they accounted for the time/temperature dependence by considering relative changes in free volume at the T_g.

One important factor which is often overlooked in relaxation studies on polymers is the polydispersity index. Adachi et al. reported significant high-frequency broadening of dielectric loss curves for polyisoprene when the polydispersity index increased from 1.03 to 1.34.[44] Their work was concerned with the "normal" mode relaxation of polyisoprene, which probes end-to-end dipole vectors. Therefore, it is quite likely to be more sensitive to a distribution of chain ends than the segmental motions investigated by us are. Ngai et al. have investigated molecular motions in polycarbonates and adapted the coupling model to take account of a distribution of primitive relaxation times brought about by a distribution of chain lengths.[45] This was necessary for analyzing local motions, but for the α-relaxation, only an average free volume needed to be accounted for due to the volume of the molecular relaxing units being much larger then the average hole size. Fu et al., in their recent dielectric study of poly(arylene ether)s,[43] showed that dielectric loss curves broadened as polar pendant groups on the polymer backbone were added and steric hindrance increased. The differences in broadness were small, presumably due to the structural similarity of the polymers, and each polymer had a polydispersity index close to 2. In our study, the polydispersity, which varied between 2 and 3, may have exerted a strong influence on the relaxation behavior. Obviously it would be desirable to investigate polymers with as close to a monodisperse nature as possible to more precisely determine the applicability of the coupling model to the relaxation behaviour of rigid aromatic thermoplastic polymers.

The normalized relaxation strength S of the mechanical α-relaxation can be calculated from the area of the loss peak observed in temperature scans. According to Read and Williams[30] if the average activation energy is ΔE and is calculated from peak shifts, S can be calculated using

$$\int_0^\infty \tan\delta \, \mathrm{d}(1/T) = \frac{1}{2}\sum \pi R/\Delta E \qquad (9)$$

where S is the normalized strength of the transition, ΔE is the activation energy, and the left-hand side of the equation is the area of a tan δ peak plotted against reciprocal absolute temperature. Values of S for each of the polymers are listed in Table 4. The relative magnitude of S generally did not vary much with polymer structure, aside from **1a** and **3b**, which both display significantly higher values. The concept of mechanical relaxation strength has limited applicability, unlike the dielectric relaxation strength which can be related to a molecular dipole moment through intra- and intermolecular dipolar correlations.

***β*-Relaxation.** The existence of a β'-relaxation, which appears as a peak on the low-temperature side of the α-process during heating scans, has been observed in amorphous PEEK,[31] as well as in other rigid polymers, such as polyethersulfone (PES)[32] and polycarbonate.[33] Sasuga and Hagiwara consider this process in PEEK to be due to rearrangement of the main chain toward more rigid amorphous packing, since it is greatly reduced by annealing the polymer at 100 °C prior to scanning. Fried et al. attributed this process in PES to be due to intra- or interchain cooperative motions involving movement of several groups along the chain. It was also eliminated by annealing. David and Etienne,[34] in discussing this transition in PEEK, state that it is not a true relaxation, rather it due to the presence of an excess defect concentration within the glassy polymer which collapses during heating. The occurrence of β-relaxations in polyimides is well-known and they have been observed by dielectric, dynamic mechanical, and NMR techniques.[35] They have been assigned to motions of both dianhydride and diamine units.

A typical dynamic mechanical spectra showing the temperature of dependence of tan δ is shown in Figure 8 for **4a**. Note that the data presented result from a sample that had been annealed for a short period of time above the T_g in order to eliminate potential β' peaks. A weak shoulder can be seen on the low-temperature side of the main α-peak. It is fairly broad in nature, first appearing around 115 °C and eventually merging with the α-peak. Indeed, it has the appearance of the type of β' peak discussed above. Peaks very similar in shape and relative temperature location were also observed in the spectra of **2b** and **2a**, while **1a** exhibited a weak, broad peak centred around 70 °C. No superambient secondary transitions were detected in any of the remaining polymers. A structural feature common to **1a**, **2a**, and **4a** is the cyclic biphenyl group. An additional point of interest is that although **4a** and **3a** differ in structure only by the presence of a main-chain keto linkage in **3a**, no β- (or β') transitions were detected

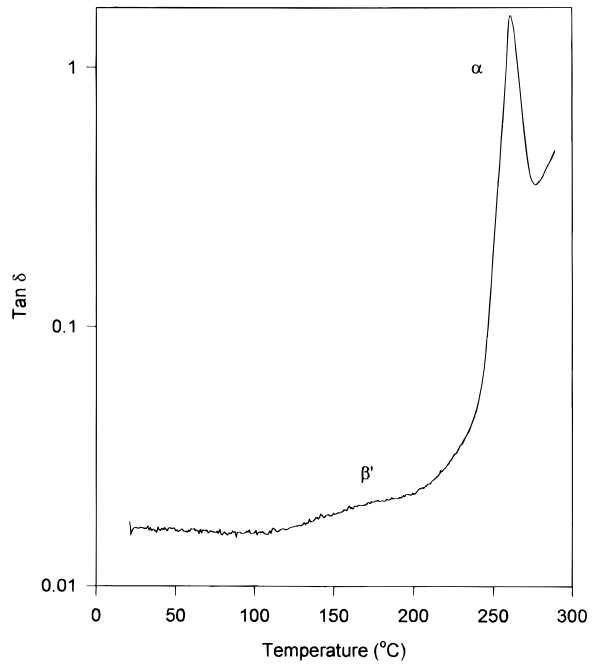

Figure 8. Temperature dependence of DMTA tan δ in β-relaxation region for **4a**.

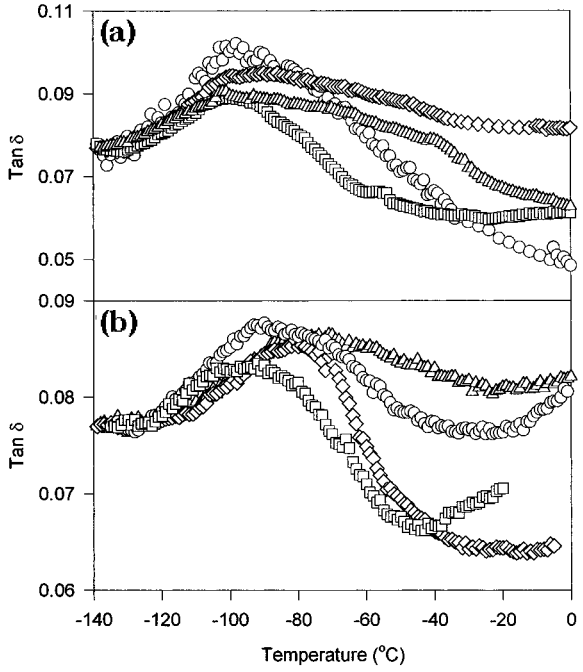

Figure 9. Temperature dependence of DMTA tan δ in γ-relaxation region. (a) non-perfluorinated polymers, (b) perfluorinated polymers: **1a** (◇), **1b** (○), **2a** (△), **2b** (□), **3a** (□), **3b** (○), **4a** (◇), **4b** (△).

in **3a**. Furthermore, no trend associated with the presence or otherwise of perfluorination is discernible.

The broadness of the β-peak in the polymers in which they were observed and their proximity to the α-peak prevents quantitative evaluation in terms of defining β-peak maximums with reasonable accuracy or peak shifts with changing frequency. Further studies are required to determine if these are true relaxation processes, rather than β'-transitions. Only a few relaxation studies on similar polymers have been carried out. For a polyketone containing phenolphthalein linkages Han et al.[36] report a broad β-process with a maximum around 140 °C. A weak transition centred around 100 °C is apparent in the dynamic mechanical spectra reported by Hendricks and Lau[37] for a perfluorinated aryl ether ketone. The complete structure of this polymer is not revealed, although its T_g is close to that of **4a**.

***γ*-Relaxation.** The origins of subambient secondary relaxations in rigid aromatic polymers has been discussed in a number of previous studies. David and Etienne[14] report that the mechanical β-process in PEEK (which occurs around −80 °C) results from the superposition of two motional processes; a low-temperature component reflects local intrachain motions, while a high-temperature cooperative component is attributed to local motions in ordered amorphous regions. Jonas and Legras[38] suggest that phenyl ring flips are responsible for the β-process and that it is sensitive to water content, aging history, and morphology. Fried et al.[32] attribute the water sensitive dynamic mechanical γ-peak in PES (at −108 °C) to a combination of motions in the isopropylidene, diphenyl sulphone, and diphenyl ether units. A bimodal γ-transition in an aromatic polyimide investigated by dielectric relaxation[39] is also reported to be sensitive to moisture content, with both components undergoing a loss in intensity with decreases in relative humidity. Wendorff et al.[40] states a general conclusion that subambient secondary relaxations in aromatic polymers are connected with intra- and intermolecular motions on a length scale equivalent to a single repeat unit.

The temperature dependence of tan δ for all poly(aryl ether ketone)s are shown in Figure 9. A number of structure related trends in the γ-transition can be seen in these plots.

Among those without perfluorophenylene linkages (Figure 9a), the presence of the cyclic biphenyl side group in **1a** and **2a** results in significant broadening and the appearance of a second component on the high temperature side of the γ-peak. This result is consistent with the two-component model of the γ-transition of David and Etienne since the bulky side group will increase the cooperativity of local motions. The temperature location of the γ-peak maximum is increased only very slightly by the cyclic biphenyl. The incorporation of an oxidiazole linking group, in place of the keto linkage, reduces the peak intensity but has little effect on peak temperature location.

Polymer **1a** was also scanned immediately after storing under vacuum at 100 °C for 1 week to investigate the effect of absorbed moisture on the γ-transition. The effect of this was to increase the peak maximum temperature from −100 °C for the "wet sample" to −90 °C for the "dry" sample at the same as reducing the intensity of the relaxation. An Arrhenius analysis of the frequency dependence of this transition revealed an activation energy of 56 ± 0.5 kJ/mol for the dry sample (compared with 54 ± 0.3 kJ/mol for the wet sample). These findings are consistent with an earlier study[38] by Jonas and Legras who report that water acts as a plasticizer for the subambient β-relaxation in PEEK, such that increasing the water content decreases the temperature location of the relaxation, decreases the activation energy, and lowers the intensity. They contend that the β-relaxation involves a cooperative motion of a PEEK segment and a water molecule. The Arrhenius activation energies for **1b**, **2b**, and **2a** were 43 ± 4, 51 ± 2 and 52 ± 2, respectively. These are typical values for sub-T_g transitions of this nature.

For those polymers containing perfluoro linkages (Figure 9b) the intensity of the γ-peak is drastically

reduced, compared with the spectra shown in Figure 9a. The effect of the stiffness of the polymer chain on the temperature location of the transition is very apparent from a comparison of the polymer pairs **3a** and **4a** and **3b** and **4b**. Removal of the keto linkage shifts the peak 20 K to higher temperatures in both cases. Thus, chain stiffness is more influential in controlling the rate of local chains motions than in controlling the incorporation of a bulky side group. This supports the idea that main-chain phenyl motions are involved in the γ-process since the rate of ring flipping will be controlled by chain stiffness.

The high temperature broadening seen in Figure 9a is also present in the spectra of **3b** and **4b**, neither of which contain cyclic biphenyl yet both contain fluorine. Fluorination of polyimides has been shown to increase free volume[41] and greater free volume may be expected to reduce the cooperative nature of local motions. If the presence of fluorine causes a similar increase in free volume in the polymers in this study, the observed broadness may arise from more complex factors than those already referred to. When both perfluoro and cyclic biphenyl are present the extent of high temperature broadening is significantly reduced.

A comparison of **1b** and **3b** shows that the peak temperature location is largely unaltered when the structure is perfluorinated. However, when perfluoronation is added to a structure that already contains cyclic biphenyl (compare **1a** with **3a**), slight plasticization occurs and the peak temperature location shifts to lower temperatures. This is accompanied by a reduction in peak broadness.

Conclusions

The glass transition temperatures of the polymers studied here, as measured by DSC and DMTA, show significant variation which can be accounted for from consideration of polymer structure. Polymers containing cyclic biphenyl side groups were found to be the most thermally stable in air. Analysis of the temperature dependence of the mechanical relaxation frequency using the WLF equation showed the polymers containing cyclic biphenyl side groups to have the highest intramolecular barriers to rotation, while incorporation of perfluorophenylene groups resulted in internal plasticization and a lowering of T_g. Polymers containing cyclic biphenyl side groups were also more intermolecularly coupled, judged by the steepness of the temperature dependence of the WLF shift factors. However, this did not correlate with the broadness of the relaxation as predicted by the coupling model.

Sub-T_g mechanical β-peaks were observed in only a few polymers, in particular those containing a cyclic biphenyl side group and who had the appearance of a structural β'-type relaxation. The γ-process was shown to be sensitive to the presence of chain structure, chain flexibility, and absorbed moisture. The data illustrated the complex relationships that determine the sub-T_g relaxation processes in polymers of this type.

Further studies on monodisperse polymers are required to more fully relate changes in molecular structure to relaxation models such as the coupling model.

References and Notes

(1) Frazer, A. H. in *Polymer Reviews*; Interscience Publishers: New York, 1968; Vol. 17, pp 159−175, High Temperature Resistant Polymers.

(2) Mittal, K., Ed. *Polyimides: Synthesis, Characterization, and Applications*; Plenum Press: New York, 1984; Vols. 1 and 2.

(3) Attwood, T. E.; Dawson, P. C.; Freeman, J. L.; Hoy, L. R. H.; Rose, J. B.; Staniland, P. A. *Polymer* **1981**, *22*, 1096.

(4) Ohno, M.; Takata, T.; Endo, T. *J. Polym. Sci., Part A: Polym. Chem.* **1995**, *33*, 2647.

(5) Hergenrother, P. M.; Jensen, B. J.; Havens, S. J. *Polymer* **1987**, *29*, 358.

(6) Rose, J. B. *Polymer* **1974**, *15*, 456.

(7) Cassidy, P. E.; Aminabhavi, T. M.; Farley, J. M. *J. Macromol. Sci., Rev. Macromol. Chem. Phys.* **1989**, *C29* (2, 3), 365.

(8) (a) Mercer, F. W.; Goodman, T. D. *Polym. Prepr.* **1991**, *32* (2), 189. (b) Mercer, F. W.; Goodman, T. D.; Wojtowicz, J.; Duff, D. *J. Polym. Sci. Part A: Polym. Chem.* **1992**, *30*, 1767.

(9) Hendricks, N. H.; Lau, K. S. Y. *Polym. Prepr.* **1996**, *37* (1), 150.

(10) Cogswell, F. N. *Thermoplastic Aromatic Polymer Composites: A Study of the Structure, Processing and Properties of Carbon Fibre Reinfored Polyetheretherketone and Related Materials*; Butterworth-Heinemann: U.K., 1992.

(11) Krishnaswamy, R. K.; Kalika, D. S. *Polymer* **1994**, *35*, 1157.

(12) Ahlborn, K. *Cryogenics* **1988**, *28*, 234.

(13) Goodwin, A. A.; Hay, J. N. *Polym. Commun.* **1989**, *30*, 288.

(14) David, L.; Etienne, S. *Macromolecules* **1992**, *25*, 4302.

(15) Mercer, F.; Goodman, T.; Woitowicz, T.; Duff, D. *J. Polym. Sci., Part A: Polym. Chem.* **1992**, *30*, 1767.

(16) Mercer, F. *Polym. Mater. Sci. Eng.* **1992**, *66*, 268.

(17) Draper, N. R.; Smith H. *Applied Regression Analysis*; 2nd ed.; Wiley: New York, 1966; p 28.

(18) St. Clair, A.; St. Clair, T.; Winfree, W. *Polym. Mater. Sci. Eng.* **1988**, *59*, 28.

(19) Hendricks, N. H. *Solid State Technol.* **1995**, *38*, 117.

(20) (a) Vogel, H. *Phys. Z.* **1921**, *22*, 645. (b) Fulcher, G. S. *J. Am. Chem. Soc.* **1925**, *38*, 339.

(21) Starkweather, H. W. *Macromolecules* **1993**, *26*, 4805.

(22) Ngai, K. L.; Roland, C. M. *Macromolecules* **1993**, *26*, 6824.

(23) Williams, M. L.; Landel, R. F.; Ferry, J. D. *J. Am. Chem. Soc.* **1955**, *77*, 3701.

(24) Ferry, J. D. *Viscoelastic Properties of Polymers*, 3rd ed.; Wiley: New York, 1980.

(25) Ngai, K. L.; Rajagopal, A. K.; Teitler, S. *J. Chem. Phys.* **1988**, *88*, 6088.

(26) Havriliak, S.; Negami, S. *Polymer* **1967**, *8*, 161.

(27) (a) Kohlrausch, F. Pogg *Ann. Phys.* **1863**, *119*, 352. (b) Williams, G.; Watts, D. C. *Trans. Faraday Soc.* **1970**, *66*, 80.

(28) Moynihan, C. T.; Boesch, L. P.; Laberge, L. *Phys. Chem. Glasses* **1973**, *14*, 122.

(29) Connolly, M.; Karasz, F.; Trimmer, M. *Macromolecules* **1995**, *28*, 1872.

(30) Read, B. E.; Williams, G. *Trans. Faraday Soc.* **1961**, *57*, 1979.

(31) Sasuga, T.; Hagiwara, M. *Polymer* **1985**, *26*, 501.

(32) Fried, J. R.; Letton, A.; Welsh, W. J. *Polymer* **1990**, *31*, 1032.

(33) Bauwens-Crowet, C.; Bauwens, J. C. *Polymer* **1990**, *31*, 646.

(34) David, L.; Etienne, S. *Macromolecules* **1993**, *26*, 4489.

(35) Cheng, S. Z. D.; Chalmers, T. M.; Gu, Y.; Yoon, Y.; Harris, F. W.; Cheng, J.; Fone, M.; Koenig, J. L. *Macromol. Chem. Phys.* **1995**, *196*, 1439.

(36) Han, Y.; Yang, Y.; Li, B.; Wang, X.; Feng, Z. *J. App. Polym. Sci.* **1995**, *57*, 655.

(37) Hendricks, N. H.; Lau, K. S. Y. *Polym. Prepr.* **1996**, *37* (1), 150.

(38) Jonas, A.; Legras, R. *Macromolecules* **1993**, *26*, 813.

(39) Zaluski, C.; Gu, X.; Yu, Q.; Wang, Z. Y. *J. Pol. Sci. B.* **1996**, *34*, 731.

(40) Schartel, B.; Wendorff, J. H. *Polymer* **1995**, *36*, 899.

(41) Hougham, G.; Tesoro, G.; Viehbeck, A. *Macromolecules* **1996**, *29*, 3453

(42) Soliman, M.; Wendorff, J. H.; Winter, H. *Proceedings of the 5th European Symposium on Polymer Blends*; p 269.

(43) Fu, C. Y. S.; Lackritz, H. S.; Priddy, D. B., Jr.; McGrath, J. E. *Chem. Mater.* **1996**, *8*, 514.

(44) Adachi, K.; Kotaka, K. *Prog. Polym. Sci.* **1993**, *18*, 585.

(45) Ngai, K.; Rendell, R. W.; Yee, A. F. *Macromolecules* **1988**, *21*, 3396.

MA9606768